

1-1-2012

## Proton beam characterisation of a prototype thin-tile plastic scintillator detector with SiPM readout for use in fast-neutron tracker

R Preston  
*University of Wollongong, rmp987@uowmail.edu.au*

J Jakubek  
*Czech Technical University in Prague*

Dale A. Prokopovich  
*ANSTO, dap11@uow.edu.au*

J Uher  
*CSIRO Lucas Heights*

Follow this and additional works at: <https://ro.uow.edu.au/engpapers>



Part of the [Engineering Commons](#)

<https://ro.uow.edu.au/engpapers/4596>

---

### Recommended Citation

Preston, R; Jakubek, J; Prokopovich, Dale A.; and Uher, J: Proton beam characterisation of a prototype thin-tile plastic scintillator detector with SiPM readout for use in fast-neutron tracker 2012, 1-14.  
<https://ro.uow.edu.au/engpapers/4596>

# Proton Beam Characterisation of a Prototype Thin-Tile Plastic Scintillator Detector with SiPM Readout for use in Fast-Neutron Tracker

---

Rhys Preston<sup>a,b\*</sup>, Jan Jakubek<sup>c</sup>, Dale Prokopovich<sup>d</sup> and Josef Uher<sup>a</sup>

<sup>a</sup> *CSIRO Process Science and Engineering & CSIRO Minerals Down Under Research Flagship  
Lucas Heights, Australia*

<sup>b</sup> *Centre for Medical Radiation Physics, University of Wollongong,  
Wollongong, Australia*

<sup>c</sup> *Institute of Experimental and Applied Physics, Czech Technical University,  
Prague, Czech Republic*

<sup>d</sup> *Institute of Materials Engineering, Australian Nuclear Science and Technology Organisation,  
Lucas Heights, Australia*

E-mail: [rhys.preston@csiro.au](mailto:rhys.preston@csiro.au)

**ABSTRACT:** We present details of the construction and characterisation of a prototype thin-tile plastic scintillation detector for use in a multi-layer Fast Neutron Tracker. Scintillation light is read out using solid-state silicon photomultiplier detectors (SiPMs). The Tracker consists of alternating scintillator and Timepix detector layers. The scintillator tile provides a hydrogen-rich target, in which impinging fast neutrons produce recoil protons. The energy lost by protons in the plastic scintillator are measured and recoil protons exiting the scintillator are tracked in the Timepix detector. The combination of signals from the scintillator and Timepix provides information to reconstruct the energy or direction of the impinging neutron, using calculations based on the kinematics of the elastic neutron scattering.

Three prototype scintillation detectors were constructed, using either a pair of 3x3 mm sensitive area SPMMicro3035 SiPMs from SensL or a pair of MAPD-3n SiPMs from Zecotek. The detector performances were characterised using a mono-energetic proton beam. An absolute energy calibration was measured at 3, 4 and 5 MeV proton energies with good linearity. The best measured energy resolution was 29.8% at 5 MeV. Spatial uniformity was assessed by measuring the response across the detector face. Finally, the tile detector's ability to provide a trigger for Timepix acquisition in the stack configuration was demonstrated for single and double neutron recoil events using a DT neutron source. The SiPM-based design was found to be well-suited for the application of the multi-layer fast neutron tracker.

**KEYWORDS:** Neutron detectors (cold, thermal, fast neutrons); Particle tracking detectors; Optical detector readout concepts

---

\* Corresponding author.

---

## Contents

<b>1. Introduction</b>	<b>1</b>
<b>2. SiPM-Based Plastic Scintillator Tile Detector</b>	<b>2</b>
2.1 Detector Design	2
2.2 Electronic Readout and Processing	3
<b>3. Device Characterisation using Protons</b>	<b>5</b>
3.1 The ANTARES Heavy Ion Microprobe	5
3.2 Anti-Coincidence Noise Rejection	5
3.3 Energy Calibration and Resolution	6
3.4 Detector Spatial Uniformity	9
<b>4. Detector Test with DT Neutrons</b>	<b>9</b>
4.1 Dual Layer Stack and Triggering Setup	9
4.2 Double Recoil Coincidence	11
4.3 DT Energy Spectra	12
<b>5. Conclusions and Future Work</b>	<b>14</b>

---

## 1. Introduction

A Fast Neutron Tracker capable of measuring the energy and direction of fast neutrons is under development. This detector is based on a scalable multi-layer design with plastic scintillator tiles read out using silicon photomultipliers (SiPM). The tiles are interleaved with Timepix detectors (Figure 1). Timepix is a single-quantum counting silicon detector. Charge pairs produced by ionisation in the silicon layer are collected and digitised by an array of 256x256 readout channels with a pitch of 55  $\mu\text{m}$  [1]. Data acquisition with the Timepix is triggered by a signal from the appropriate scintillator.

If a fast neutron collides with a proton in the plastic scintillator, there is a certain probability that the proton escapes from the plastic and enters the Timepix pixel detector where its ionisation track is recorded. The scattered neutron can pass through the Timepix and further recoil another proton in the scintillator of the next Scintillator + Timepix detector pair. Analysis of the proton tracks in the Timepix devices and the energies that the protons lose in the plastic scintillators allows calculation of the energy and direction of the original neutron [2], [3].

The multilayer design requires a highly compact optical detector for the readout of the scintillation light. Silicon photomultipliers (SiPM) are solid-state optical photon detectors with a high internal gain that provides tolerance to electronic noise and allows use of relatively simple readout electronics [4], [5].

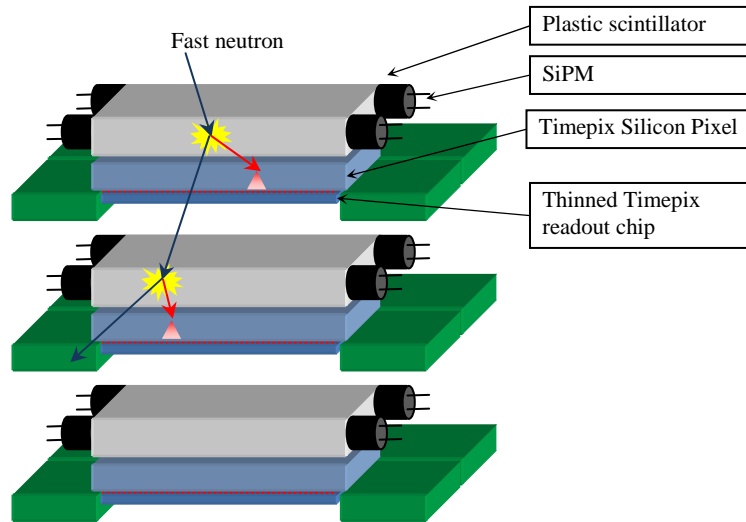


**Figure 1: Schematic of neutron tracking detector concept with alternate layers of plastic scintillator and pixellated, charge-sensitive detectors.**

This paper presents the results for the first prototype of a tile detector with SiPM readout for use in the Fast Neutron Tracker. The energy resolution, linearity and spatial uniformity of the detector's response were characterised using a proton beam of selectable energy from the ANTARES Heavy Ion Microprobe at ANSTO, Lucas Heights, Australia [6]. Single and multiple neutron recoil events were collected in a multilayer detector configuration using 14 MeV neutrons from a Deuterium-Tritium (DT) neutron generator operated at CSIRO PSE, Lucas Heights, Australia.

## 2. SiPM-Based Plastic Scintillator Tile Detector

### 2.1 Detector Design

The first prototype used a 15x15x2 mm EJ-204 plastic scintillator tile from Eljen [7]. EJ-204 is a Polyvinyl Toluene (PVT) based scintillator with a fast 1.8 ns decay time. The 15x15 mm area of the scintillator was chosen to cover the 14x14 mm sensitive area of the Timepix detector. The thickness was 2 mm, as protons recoiled by 14 MeV neutrons from a thicker plastic scintillator would be less likely to exit the scintillator and reach the underlying Timepix device. The CSDA (constant slowing down approximation) range of protons in PVT plastic scintillators is 0.35 mm at 5 MeV and 2.16 mm at 14 MeV [8]. Trapezoidal Perspex light guides of 10 mm length were attached on opposing 15x2 mm faces with optically transparent epoxy. The cross-sectional areas of the light guides varied from 15x3 mm at the input end to 3x3 mm at the output end as shown in Figure 2. SiPMs with an active area of 3x3 mm were coupled to the light guide ends using General Electric RTV615 optically transparent silicone. The light guides were painted with a titanium dioxide-based white acrylic paint to reduce light loss. The scintillator plates were left unpainted. Paint would reduce the energy of recoiled protons after exiting the scintillator or even stop them completely. It would have a similar effect on protons from the accelerator used for the scintillator characterisation and calibration.

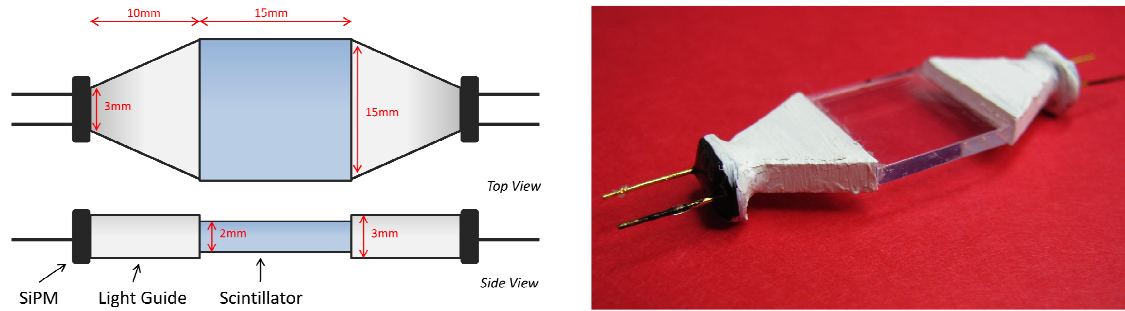


**Figure 2: The prototype neutron recoil detector design used dual SiPMs coupled via light guides to opposite sides of a plastic scintillator.**

Three such detectors were constructed, two with dual SensL SPMMicro3035 SiPMs [9] (abbreviated S3035) and one with dual Zecotek MAPD-3n SiPMs [10], [11]. One pair of S3035 and the pair of MAPD-3n SiPMs were closely matched in breakdown voltage. This allowed the SiPMs to be run at almost the same voltage above breakdown (over-bias), and hence similar gain, from a common bias voltage supply.

The SiPMs were run at 2 V over-bias. The MAPD-3n devices, with specified  $86.41 \pm 0.005$  V and  $86.42 \pm 0.005$  V breakdown voltages, were run at 88.42 V. The matched S3035 devices, both with  $26.66 \pm 0.005$  V breakdown voltages, were biased at 28.66 V. The final S3035 pair, with  $27.45 \pm 0.005$  V and  $27.13 \pm 0.005$  V breakdown voltages, were biased separately at 29.45 V and 29.13 V.

## 2.2 Electronic Readout and Processing

The detectors were mounted directly above the Timepix sensor surface. The SiPM leads were connected to a bias de-coupling and signal circuit mounted on the Timepix support board via 4 cm of wire, minimising electronic noise pick-up from the Timepix and from external sources. The circuit is shown in Figure 3.

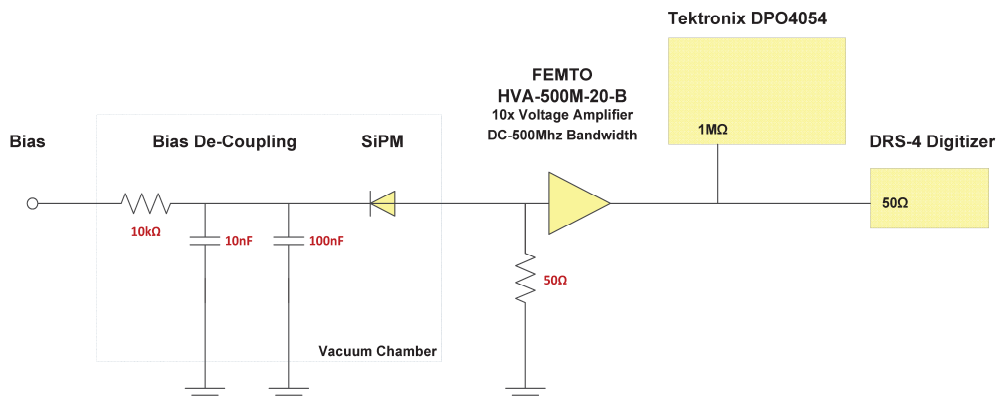


**Figure 3: Electronics for SiPM biasing and readout**

The SiPM signals were transmitted from the board using 50  $\Omega$  co-axial cables to FEMTO HVA-500M-20-B 500MHz DC coupled 10x gain non-inverting voltage amplifiers [12]. The amplified signals were digitised using a DRS-4 Evaluation Board [13]. The DRS-4 provides analogue sampling of a signal at rates between 1 and 5 GSps using a capacitive array. When a trigger signal is received by the DRS-4, the charges stored in the capacitor array are digitised using a 14 bit ADC running at a 33 MSps sampling rate. The SiPM pulses were sampled at 1 GSps, allowing up to 50 traces with length of 1024 samples to be recorded per second, which is a reasonable match for the  $<100/s$  event rate from the proton beam. The AC-coupled front-end of the DRS-4 board has a bandwidth of 200 MHz. The data was downloaded from the DRS-4 over a USB link and recorded to a binary file on the host PC.

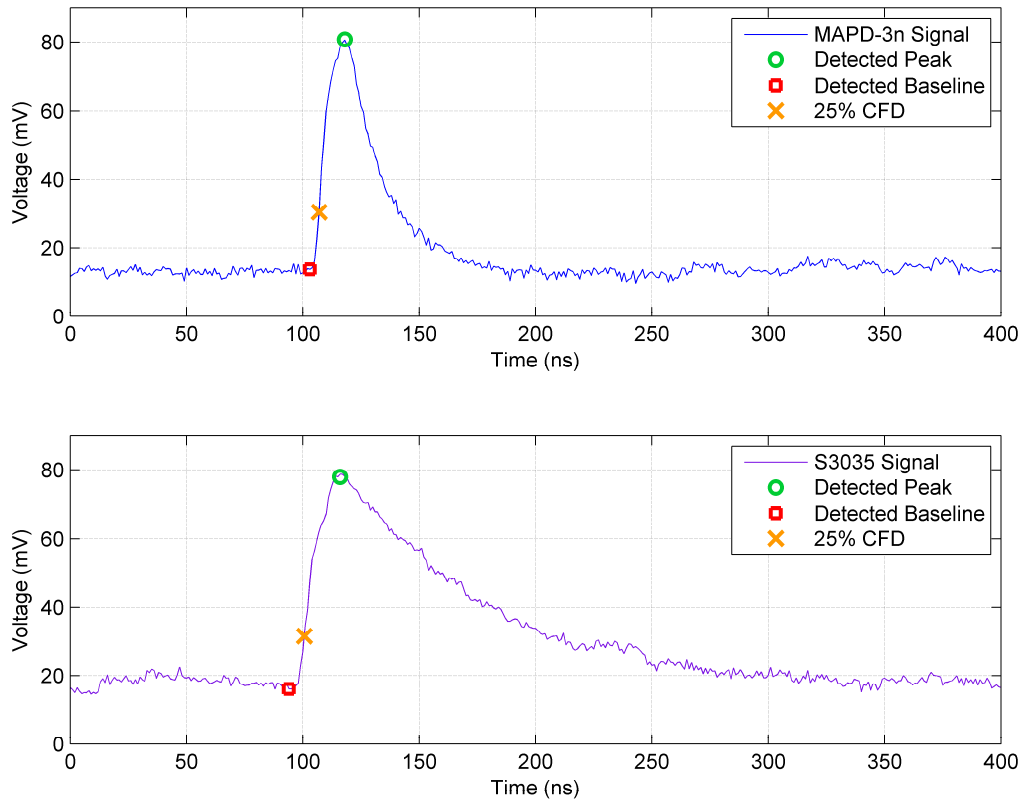


**Figure 4: Example pre-amplified pulses, from scintillations due to 5 MeV protons, from the MAPD-3n (upper) and S3035-based detectors (lower). The software-based DPP measures the relative height of the pulse above the baseline. Pulse timing is measured on the fast rising edge.**

Digital pulse processing (DPP) was performed offline. The pulse processing algorithm works as follows. Each trace was scanned for its maximum value. The baseline ahead of the pulse was located by scanning the numerically differentiated signal for the zero-crossing. The baseline level was subtracted from the maximum value, correcting for baseline disturbances arising from either the effects of AC coupling or from SiPM dark noise.

The arrival time of the pulse was estimated using a numerical implementation of a constant fraction discriminator, by interpolating the time where the rapidly rising pulse-edge reached a fraction of the final pulse height. An example pulse with the measured pulse maximum, baseline and 25% constant fraction discriminator (CFD) time is shown in Figure 4.

### **3. Device Characterisation using Protons**

#### **3.1 The ANTARES Heavy Ion Microprobe**

It is difficult to assess, with fast neutrons, the energy calibration and resolution of scintillation detectors designed for the detection of fast neutrons. Fast neutrons primarily interact through inducing proton recoils. The energy of the recoiling protons depends on the scattering angle, giving rise to a generally featureless pulse height spectrum [14]. Characterisation of plastic scintillators with gamma-ray spectroscopy is not ideal, as scintillators respond differently to photons and particles due to differing ionisation densities [15]. Furthermore due to the low average atomic number of plastic scintillators, it is difficult to obtain a discernible photo-peak from organic scintillators in gamma spectroscopy.

To avoid these difficulties, the performance of the scintillator detectors was measured using protons at the Heavy Ion Microprobe facility at ANSTO. The ANTARES tandem-accelerator facility provides a proton beam with a selectable energy of up to 5 MeV and an energy stability of better than 0.1% [6]. The beam size when focused on the scintillator was of order of 1  $\mu\text{m}$ . The beam is well suited for testing the energy resolution, linearity and response uniformity of the scintillators.

Each detector was tested using 3, 4 and 5 MeV proton beams. To assess the uniformity of response, the beam was measured at four positions on the face of the detector. Digitiser acquisition in the DRS-4 was triggered internally by one of the SiPM channels.

#### **3.2 Anti-Coincidence Noise Rejection**

The scintillation light is produced isotropically and so is expected to be approximately shared between the two SiPMs. Trigger events not associated with scintillation were rejected in the post processing by requiring coincidence between the SiPM channels [16]. The timing resolution between the two SiPMs, as used for anti-coincidence noise rejection, was assessed by fitting a Gaussian to the histogram of measured timing delays between the two channels. The best timing resolution was achieved with the CFD level of 25%, providing a typical coincidence resolution of 1.7 ns full-width-at-half-maximum (FWHM) for both SiPM types, as shown in Figure 5.

Noise rejection was particularly useful in the lower proton energy measurements, where the trigger level had to be set very low. Some SiPM dark pulses could then also trigger the digitiser, as shown in Figure 5. In such cases the rejected noise pulses accounted for up to 60% of the total count rate. In this way, implementing coincidence in a neutron tracker will reduce the minimum necessary energy deposited for a successful detection in each scintillator.

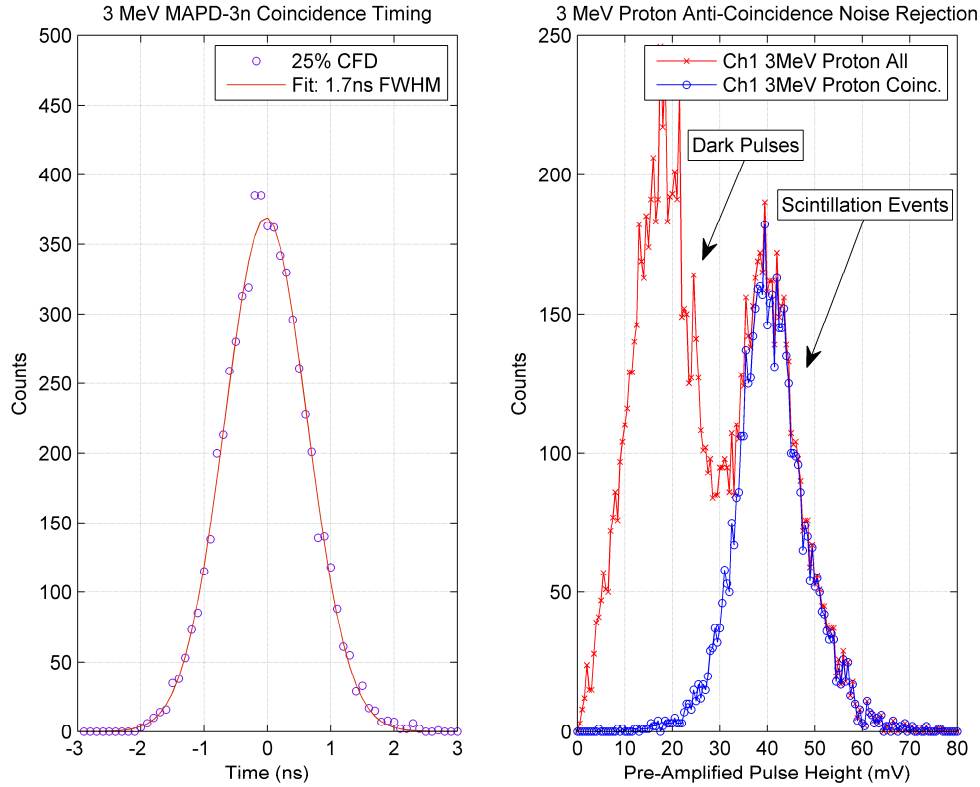


**Figure 5: Timing delay between the two SiPMs on the MAPD-3n based detector (left). Restricting the delay to a 4ns wide window allowed for the rejection of non-scintillation noise pulses (right).**

### 3.3 Energy Calibration and Resolution

The mono-energetic proton beam was used to derive an energy calibration of the scintillators and to characterise their energy resolution. The energy calibrations are shown in Figure 6 and the measured spectra for 5 MeV protons are shown in Figure 7. The detector absolute energy calibration and resolutions measurements are summarised in Table 1. The spectral peak was fitted with a Gaussian to assess the mean pre-amplified pulse height and FWHM. Resolution is expressed as the ratio of FWHM to the mean. The asymmetry of the spectral peaks may be attributed to the effects of SiPM crosstalk [17].

Both detectors exhibited good energy linearity within the limits of the measurement. As the SensL 3035 has 3640 sub pixels, the lack of significant saturation suggests that there are less than  $\sim 1000$  photons triggering microcells on each SiPM. MAPD-3n measurements at 3 MeV were discarded because the SiPM-guide coupling was damaged through contact with mounts inside the chamber. The detector was repaired for subsequent 4 MeV and 5 MeV measurements.



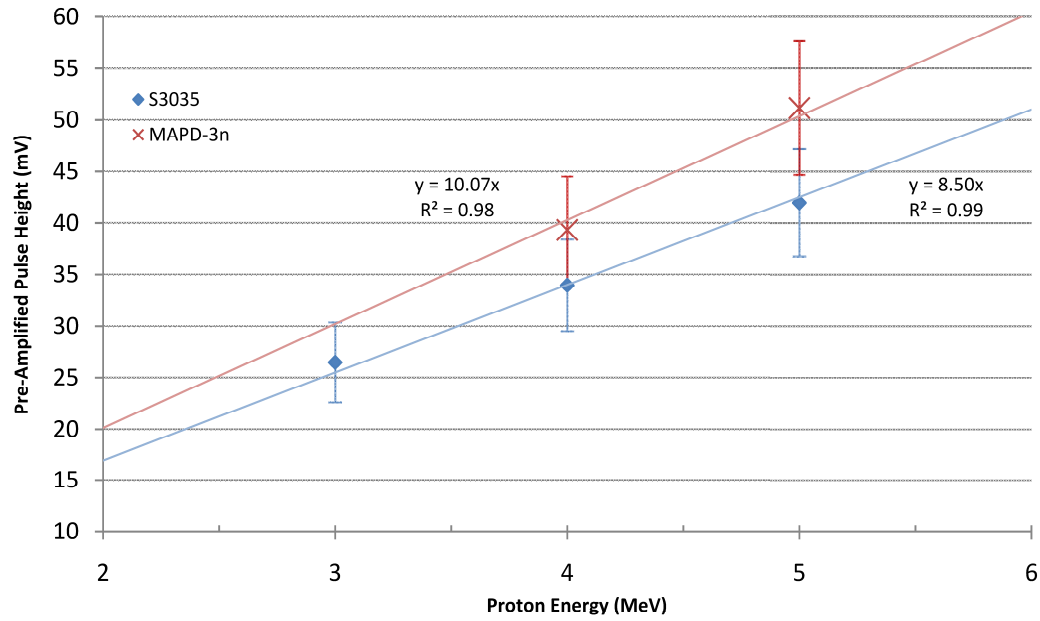


**Figure 6: Absolute energy calibration of the S3035 and MAPD-3n based detectors. The error bars indicate the standard deviation, as calculated from the fitted Gaussian. The shown linear fits are forced to intersect the origin.**

**Table 1: Absolute Energy Calibration Data**

Detector	Energy (MeV)	Ch1		Ch2		Ch 1 & 2 Average	
		Mean (mV)	Res (%)	Mean (mV)	Res (%)	Mean (mV)	Res (%)
S3035	3	29.1	41.9	23.9	59.0	26.7	34.9
	4	34.1	39.0	26	56.2	30.2	32.5
	5	45.2	40.5	43.6	44.3	44.6	29.8
MAPD-3n	4	40.3	35.5	38.4	50.0	39.3	31.1
	5	50.4	38.7	51.8	44.8	51.2	29.8
Matched S3035	5	53.5	46.5	52.2	47.1	53.1	33.7

Averaging the pulse heights from the separate SiPMs results in a resolution improvement, averaged over all measurements, of  $1.43 \pm 0.03$ ,  $1.42 \pm 0.03$  and  $1.42 \pm 0.02$  times for the S3035, matched S3035 and MAPD-3n detectors respectively. This indicated that the resolution is primarily due to random noise, where averaging over the two detectors results in a theoretical  $\sqrt{2} \approx 1.414$  improvement in resolution.

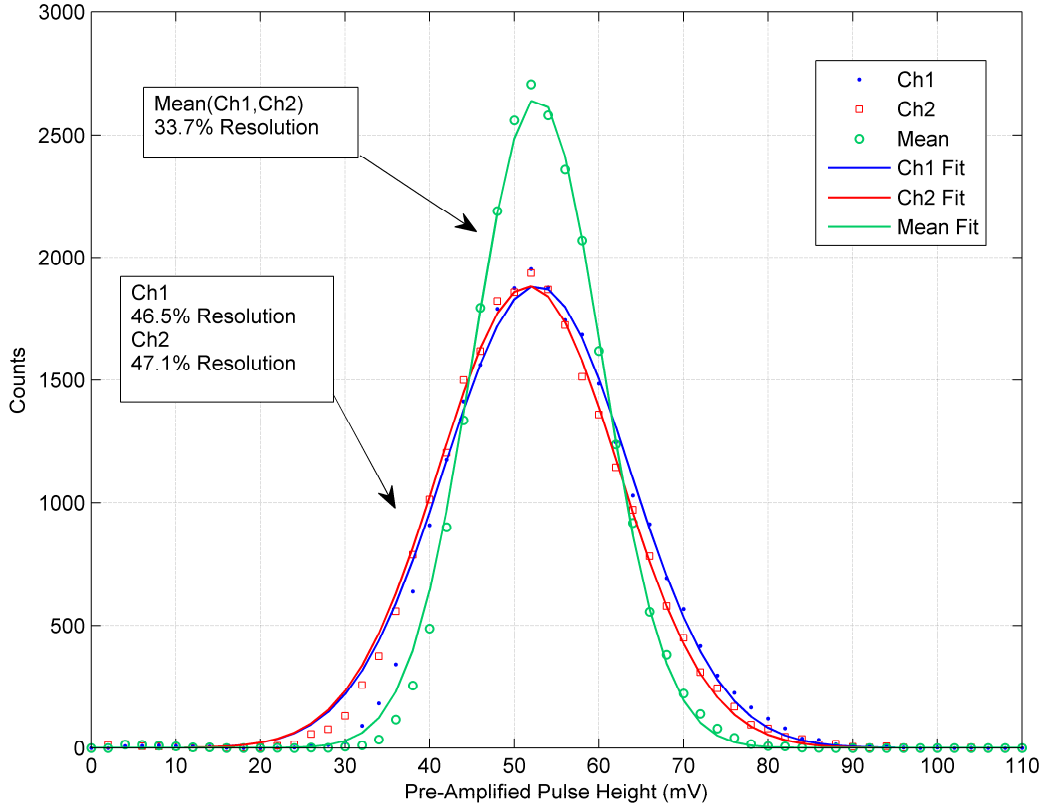


**Figure 7: Taking the mean of pulse heights from both channels provides an improvement in resolution, shown above for the Matched S3035 detector irradiated with 5MeV protons.**

Assuming that the energy resolution is dominated by Poisson statistics, the mean number of photons detected,  $\bar{n}$ , may be estimated using the measured energy resolution  $R$  [18]:

$$R = \frac{FWHM}{\bar{n}} = \frac{2\sqrt{2\ln 2} \times \sigma}{\bar{n}} \approx \frac{2.35}{\sqrt{\bar{n}}}$$

Where  $\sigma$  is the standard deviation of the Poisson distribution and equal to  $\sqrt{\bar{n}}$ . Using the data collected with the matched S3035, it was estimated that the two SiPMs were detecting  $5.4 \pm 0.2$  photons/MeV and  $5.5 \pm 0.8$  photons/MeV respectively. Additionally, analysis of the preamplified S3035 1, 2 and 3 photon dark noise pulse heights gave a 1.9 mV/photon calibration. Assuming linearity, the mean pulse height from the 5MeV protons provides agreeing values of  $5.5 \pm 0.1$  photons/MeV and  $5.6 \pm 0.1$  photons/MeV.

The S3035 effective Photo Detection Efficiency (PDE) for EJ-204 scintillation light was estimated by integrating the PDE response curve, corrected for crosstalk and dark noise [19], over the normalised scintillation wavelength spectrum [7]. The resulting efficiency is approximately 2%, meaning that there are about 550 photons/MeV striking the SiPMs. The quoted EJ-204 scintillation yield is 10400 photons/MeV for electrons. In organic scintillators, the scintillation yield for protons is less than electrons of the same energy. Using a 0.4 proton to electron response ratio, measured at 5 MeV for NE-102 in [15], the 5 MeV proton yield is

estimated to be 4160 photons/MeV. As such, only about 13% of the scintillation photons are reaching the detectors. The low light collection efficiency is attributed to the detector geometry and the lack of reflective wrappings around the scintillator.

Potential improvement in light collection efficiency will benefit both the energy resolution and neutron detection efficiency of the detector. Counting more photons in an event will reduce the contribution of Poisson statistics to energy resolution. Improved light collection will also allow smaller amounts of energy deposited in the scintillator to be detected above the SiPM dark noise. This allows the detection of fast neutron interactions closer to the scintillator surface and at smaller recoil angles.

### 3.4 Detector Spatial Uniformity

The spatial uniformity of the scintillator detector response was assessed by recording the mean pulse height at four set locations across the face of each detector at a fixed proton energy. The uniformity was quantified as the ratio of the standard deviation of these measurements to the overall mean and is shown in Table 2. Painting the light guides improved the uniformity of the Matched S3035 detector from 8.7% to 4.2% and improved the signal by 25%.

**Table 2: Assessment of Spatial Uniformity of Response for Each Detector Variant**

Detector	Energy (MeV)	Light Guides	Mean Pulse Height at Location				Uniformity (%)
			Centre (mV)	Mid Top Edge (mV)	Top Left Corner (mV)	Mid Left Edge (mV)	
S3035	5	Painted	42.2	44.8	48.4	46.8	<b>5.9</b>
MAPD-3n	4	Painted	39.3	42.4	42.4	44.3	<b>4.9</b>
Matched S3035	5	Un-Painted	37.0	45.5	42.2	40.1	<b>8.7</b>
Matched S3035	5	Painted	53.1	55.4	52.1	50.2	<b>4.2</b>

It should be noted that in the complete neutron tracker, any residual lack of uniformity can be corrected for on an event-by-event basis, as the Timepix detector provides information on the location of the proton produced in the scintillator.

## 4. Detector Test with DT Neutrons

### 4.1 Dual Layer Stack and Triggering Setup

A sealed-tube neutron generator (model A-325, used with an A-3062 DT tube, both manufactured by Thermo Fisher) was used to measure neutron recoils in a 2-layer neutron tracker. The neutron generator emits approximately mono-energetic 14 MeV neutrons and the emission is nearly isotropic. The distance between the DT generator target and the detector was 55 cm, meaning that the scintillators subtended an angle of  $7.4 \cdot 10^{-4}$  steradians at the neutron emission point and thus the beam was assumed to be approximately non-divergent. The detector was constructed from the two S3035 SiPM-based scintillation detectors previously characterised and two Timepix devices. The spacing between the two scintillator tiles was 0.8 cm. The detector setup is shown in Figure 8.

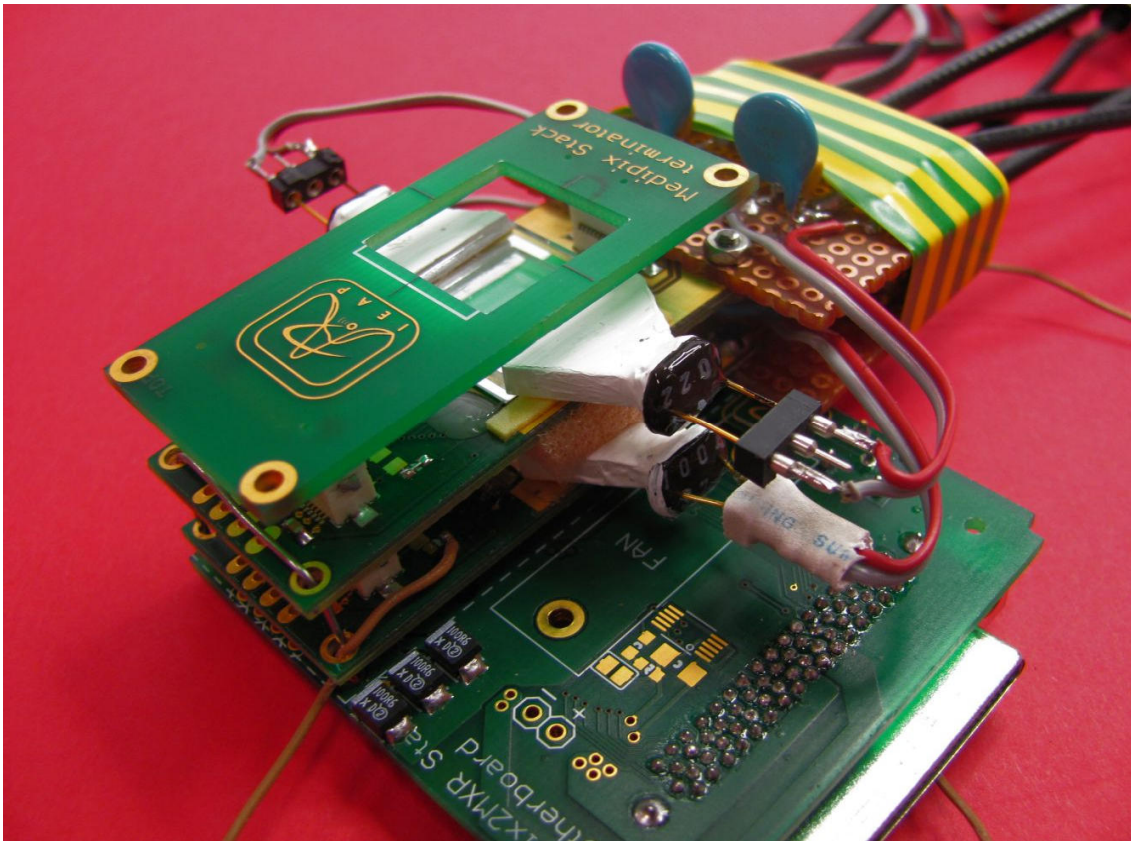


**Figure 8: The 2-layer detector stack consisting of two Timepix devices and the two SiPM-based tile scintillator detectors.**

Both SiPMs on each scintillator were read out in parallel, as shown in Figure 9. The preamplifier outputs were split between the DRS-4 digitiser input and a triggering and coincidence system using a 50 ohm balanced splitter. The triggering system was configured from conventional NIM-modules and is illustrated in Figure 10. This provided both the DRS-4 and Timepix with a common trigger when an event of sufficient energy was detected in the either of the scintillators. A signal requiring coincidence between both scintillators was also generated in order to select only double-recoil events, from which a full reconstruction of the original neutron's energy and direction is possible. Finally, a fixed-time trigger inhibit ensured synchronisation between the digitiser and the Timepix data.

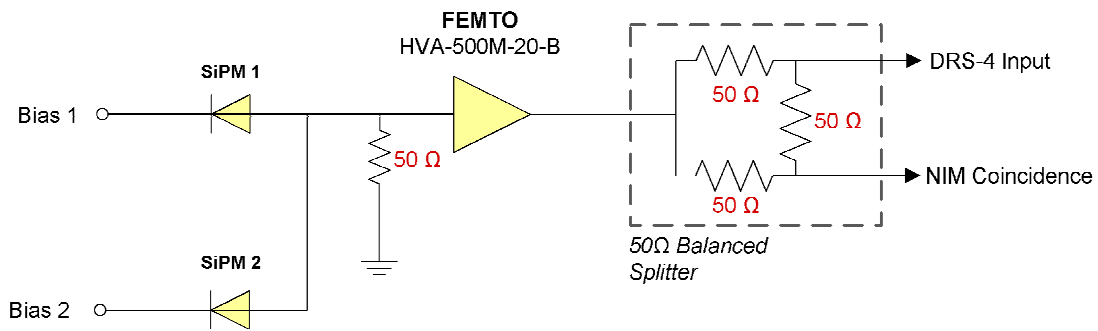


**Figure 9: Parallel SiPM readout for a single tile in dual-layer stack measurements**

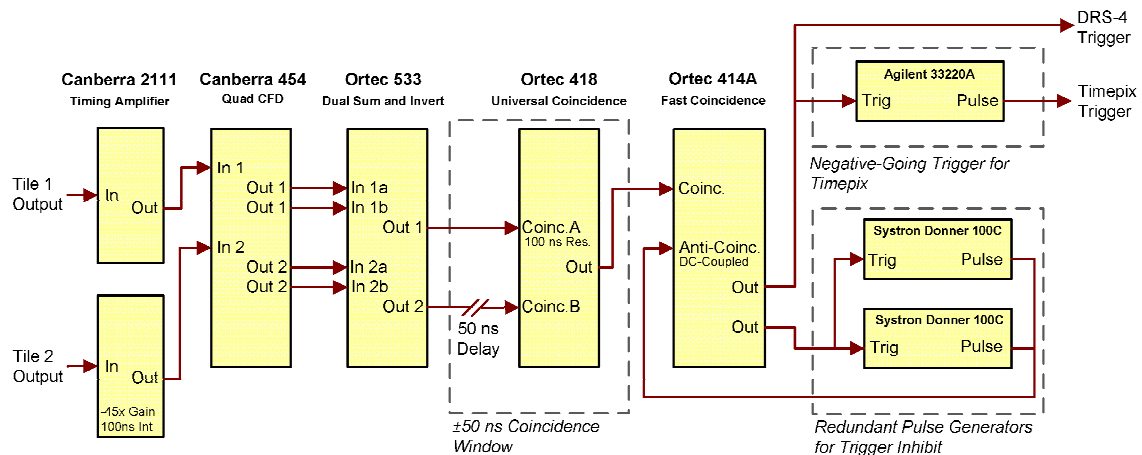


**Figure 10: NIM module-based coincidence and triggering setup for 2-layer stack measurements.**

#### 4.2 Double Recoil Coincidence

The coincidence and timing setup was first tested using a pulse generator feeding the two preamps using a 50  $\Omega$  balanced splitter. The delay histogram due to coincident 1 mV, 5 ns rise-time pulses at each preamp input exhibited a timing peak of 0.5 ns FWHM, shown in Figure 11.

The timing spectrum of the measured delay between the two detectors, using a 25% CFD, exhibits a peak with 2.7 ns FWHM (Figure 11). The distribution of transit times for scattered neutrons travelling between the scintillator tiles was calculated. This was based on the fast-neutron double-recoils possible within the geometry of the detectors and neutron source. The distribution of transit times lay between 0.15 ns and 1.16 ns, with a 0.3 ns FWHM. This made a relatively small contribution to timing spread. As such, the measured system timing resolution was 2.7 ns FWHM for coincidence between two tile detectors, or 1.9 ns FWHM resolution for a single detector.

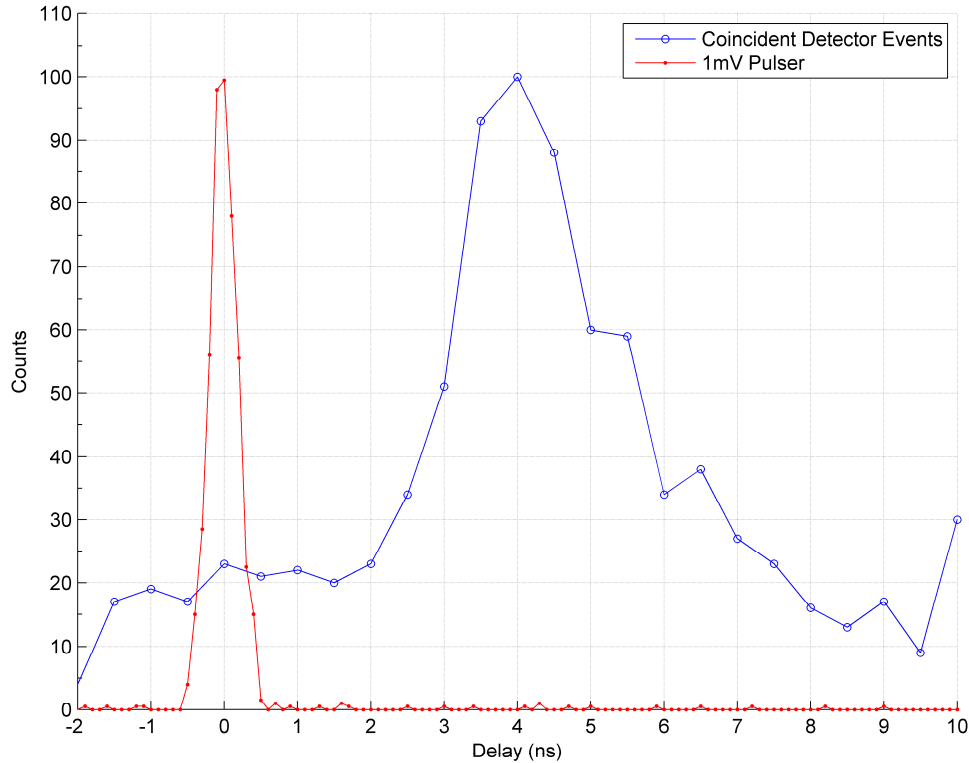


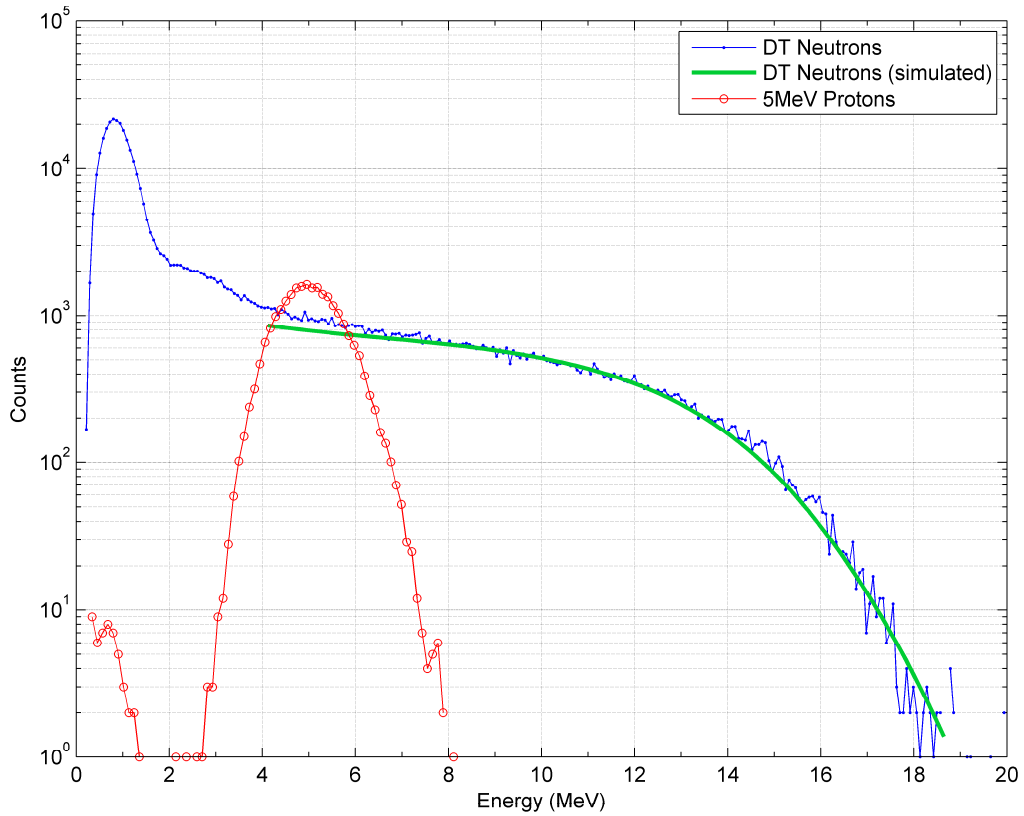
**Figure 11: Time delay spectrum from coincident triggers between the two scintillator tiles. The delay offset of the coincidence is due to differences in cable lengths.**

### 4.3 DT Energy Spectra

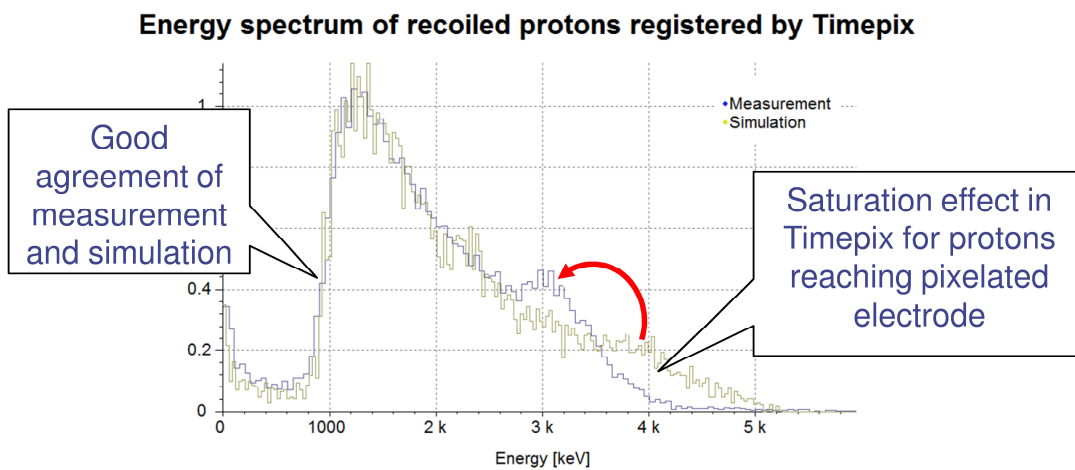
The hydrogen-recoiled protons have a uniform energy spectrum from zero energy up to the energy of incoming neutrons (14 MeV) [14]. However, some of the protons are not entirely stopped in the detector and deposit only part of their energy. This, together with limited energy resolution of the detector leads to a non-flat energy spectrum [2], [3].

Figure 12 shows the measured DT neutron spectrum compared with a result from a Monte-Carlo simulation, which simulated the elastic neutron collisions with protons in the plastic converter and the following proton transport. The code was written in C++ with geometry and tracking based on the ROOT package [20]. Details of the simulation are published in [3]. The simulated spectrum was post-processed with a variable Poisson blurring, using the calculated 11.1 photons/MeV, to account for the detector resolution. A good agreement was found between the simulated and measured spectrum above 4.5 MeV. Below this energy the measurement differs from the simulation primarily due to un-simulated carbon recoils and SiPM dark noise events.

The measured and simulated proton spectrum in the Timepix device is shown in Figure 13. The figure shows very good agreement between simulation and measurement. The only difference was registered for protons with energies close to 4 MeV. These protons reach the pixellated electrode of the 150  $\mu\text{m}$  thick Timepix sensor bringing the position of maximum ionisation density (Bragg peak) very close to the electrode. That causes saturation of the Timepix detector and leads to distortion of the spectra as indicated in the image [21].



**Figure 12: Experimental and simulated spectra of protons recoiled by 14 MeV neutrons. The experimental spectrum was measured with the plastic scintillator tile with S3035 SiPMs and calibrated from the corresponding 5 MeV proton data. Counts above 14 MeV are due to the energy resolution of the detector.**



**Figure 13: Spectrum of protons measured in the Timepix detector compared with simulation [21].**

## 5. Conclusions and Future Work

A plastic scintillator tile-based fast neutron detector was successfully characterised using a mono-energetic proton beam operated at 3, 4 and 5 MeV. The ANTARES IBIC proton beam was found to be well-suited for characterising fast neutron detectors, allowing for absolute energy calibration and an assessment of detector resolution and uniformity.

The SiPM readout of the scintillator allowed spectroscopic and timing information to be determined from each event. The detectors had a linear response within the measured energy range. The energy resolution at 5 MeV was found to be 29.8% and 32.6% for two separate S3035-based detectors and 29.8% for the MAPD-3n detector. The spatial response uniformity was measured to be 4.2% for the detector with breakdown-matched S3035 SiPMs.

Finally, the prototype detectors were successfully used in a multi-layer neutron tracker configuration to measure 14 MeV fast neutron recoil events. The scintillators were used to trigger data acquisition in a Timepix detector and to measure the energy lost by the recoiling protons in the plastic scintillator. In addition, the option of triggering only on double recoil events was tested. Timing resolution between two tile detectors was measured to be 2.7 ns for double recoil events.

The SiPM-based scintillator detector proved promising for the implementation of a multi-layer neutron tracker. Both SiPM models demonstrated the necessary low light detection and low noise characteristics for the application. However, in the current prototype design, only ~13% of the scintillation photons reach the SiPMs. There is an opportunity to significantly improve the energy resolution and lower the minimum detectable proton energy by increasing the light collection efficiency of the detector. This will be the major focus of our future work.

One way to improve the light collection efficiency is to use a large-area SiPM array to cover the top surface of the scintillator tile, or to use a linear SiPM array across two or more edges of the scintillator. Thin films of reflector deposited on the scintillator surface will also be investigated.

## Acknowledgements

We thank John E. Eberhardt for his assistance in the construction and operation of the prototype tile detector.

This work has been carried out in the framework of the CERN Medipix Collaboration.

## References

- [1] X. Llopart, R. Ballabriga, M. Campbell, L. Tlustos, W. Wong, *Timepix, a 65k programmable pixel readout chip for arrival time, energy and/or photon counting measurements*, [Nucl. Instrum. Meth. A 581 \(2007\) 485](#).
- [2] J. Uher, J. Jakubek, *Monte-Carlo simulation of fast neutron detection with Timepix*, [IEEE Nuclear Science Symposium Conference Record \(NSS/MIC\), 2009](#).
- [3] J. Uher, J. Jakubek, *Monte-Carlo simulation of fast neutron detection using double-scatter events in plastic scintillator and Timepix*, [IEEE Nuclear Science Symposium Conference Record \(NSS/MIC\), 2010](#).
- [4] E. Garutti, *Silicon photomultipliers for high energy physics detectors*, [2011 JINST 6 C10003](#)



- [5] P. Finocchiaro, L. Cosentino, M. Belluso, S. Billotta, G. Bonanno, and S. Di Mauro, *Features of silicon photo multipliers: precision measurements of noise, cross-talk, afterpulsing, detection efficiency*, *IEEE Trans. Nucl. Sci.* **56** (2009) 3.
- [6] R. Siegele, D. D. Cohen, and N. Dytlewski, *The ANSTO high energy heavy ion microprobe*, *Nucl. Instrum. Meth. B* **158** (1999) 31.
- [7] Eljen Technology, *EJ-204 plastic scintillator*, Datasheet, [http://www.eljentechnology.com/images/stories/Data\\_Sheets/Plastic\\_Scintillators/EJ204%20data%20sheet.pdf](http://www.eljentechnology.com/images/stories/Data_Sheets/Plastic_Scintillators/EJ204%20data%20sheet.pdf), March 2011.
- [8] M. J. Berger, J. S. Coursey, M. A. Zucker, and J. Chang, *Stopping-power and range tables for electrons, protons, and helium ions*, <http://www.nist.gov/pml/data/star/index.cfm>, August 2011.
- [9] SensL, *SPMMicro series*, Datasheet, [http://sensl.com/wp-content/uploads/2009/05/20090720\\_spmmicro\\_datasheet.pdf](http://sensl.com/wp-content/uploads/2009/05/20090720_spmmicro_datasheet.pdf), July 2009
- [10] Zecotek, *Zecotek MAPD*, White Paper, <http://www.zecotek.com/media/MAPD-WhitePaper-March-2011.pdf>, March 2011
- [11] N. Anfimova et al., *Novel micropixel avalanche photodiodes (MAPD) with super high pixel density*, *Nucl. Instrum. Meth. A* **628** (2011) 1
- [12] FEMTO, *HVA-500M-20-B*, Datasheet, [http://www.femto.de/datasheet/DE-HVA-500M-20-B\\_R4.pdf](http://www.femto.de/datasheet/DE-HVA-500M-20-B_R4.pdf), November 2011
- [13] S. Ritt, R. Dinapoli, U. Hartmann, *Application of the DRS chip for fast waveform digitizing*, *Nucl. Instrum. Meth. A* **623** (2010) 486.
- [14] G.F. Knoll, *Radiation detection and measurement*, John Willey and Sons, Inc., New York 2000.
- [15] D. Smith, R. Polk, and T. Miller. *Measurement of the response of several organic scintillators to electrons, protons and deuterons*, *Nucl. Instrum. Meth.* **64** (1968) 157.
- [16] R. Bencardino, J.E. Eberhardt, and R. Preston, *Anti-coincidence rejection of SiPM dark pulses for improved detection of low energy radiation*, *Nucl. Instrum. Meth. A* **619** (2010) 497.
- [17] S. Vinogradov, T. Vinogradova, V. Shubin, D. Shushakov, and K. Sitarsky, *Probability distribution and noise factor of solid state photomultiplier signals with cross-talk and afterpulsing*, *IEEE Nuclear Science Symposium Conference Record (NSS/MIC)*, 2009.
- [18] J.E. Turner, *Atoms, radiation and radiation protection*, WILEY-VCH Verlag GmbH & Co., 2007.
- [19] SensL, *SPM photon detection efficiency*, Technical Note, [http://sensl.com/pdfs/SPM\\_Tech\\_App\\_Notes/TN\\_PDE.pdf](http://sensl.com/pdfs/SPM_Tech_App_Notes/TN_PDE.pdf), November 2007.
- [20] R. Brun and F. Rademakers, *ROOT - an object oriented data analysis framework*, *Nucl. Instrum. Meth. A* **389** (1997) 81.
- [21] J. Jakubek, J. Uher, P. Soukup, *Fast Neutron Tracker based on 3D position sensitive semiconductor voxel detector*, *IEEE Nuclear Science Symposium Conference Record (NSS/MIC)*, 2010.